Journal of Mathematical Chemistry, Vol. 42, No. 4, November 2007 (© 2006)
DOI: 10.1007/s10910-006-9153-2

Transient response, model structure and systematic errors in hybrid respirometers: structural identifiability analysis based on OUR and DO measurements

J. Navarro-Laboulais*, F. López, J.I. Torregrosa, S.C. Cardona and A. Abad

Department of Chemical and Nuclear Engineering, Technical University of Valencia - EPSA, Paseo Viaducto 1, 03801 Alcoy (Alicante), Spain
E-mail: jnavarla@iqn.upv.es

Received 3 March 2006; revised 30 March 2006

Experimental respirometry shows oxygen uptake rate (OUR) transients which are not predicted by standard ASM models. These transients were analysed from a detailed modelling of hybrid respirometers. Structural identifiability analysis of several models based on local isomorphism transformation approach is carried out. It can be concluded that the knowledge of the OUR does not help positively on an accurate determination of biokinetic parameters. The measure of dissolved oxygen (DO) is just enough to calculate the group of identifiable parameters from the models in a calibration process. The analysis suggests to use only the DO data to avoid the systematic errors associated to OUR calculations. Furthermore, the existence of OUR transients after a precise modelling of the hybrid respirometer is deduced. The duration of these transients are the result of the coupling between the kinetics of the biological process and the residence time in the respiration chamber of the instrument. An expression for the duration of these transients is proposed.

KEY WORDS: Respirometry, structural identifiability, oxygen mass transfer, Monod's model, wastewaters, oxygen uptake rate

1. Introduction

Respirometry is an experimental technique that allows the determination of biokinetic parameters to model the dynamics of activated sludge processes and control the WWTP's [1–3]. The technique is based on the calculation of the oxygen uptake rate (OUR) deduced from the measurement of the oxygen in the gas or liquid phase and then, fitting these data to a Monod-like non-linear autonomous dynamic model. Thus, a respirometer should be considered basically as a measuring device conceived for OUR determination in wastewaters.

*Corresponding author.

For the purposes of the discussion presented in this paper, the errors in OUR measurement, ε_R, could be expressed as the absolute value of the difference between the OUR observed value, R_{obs}, and a model value, R_{mod}, as:

$$\varepsilon_R(\mathbf{p}, t) = |R_{obs} - R_{mod}| = \varepsilon_{sys}(\mathbf{p}, t) + \varepsilon_{ins}(\cdot, t) + \varepsilon_{rnd}(\cdot, t), \quad (1)$$

where $\varepsilon_R(\mathbf{p}, t)$ is the residual error of the OUR, and $\varepsilon_{sys}(\mathbf{p}, t)$ is the systematic error attributed to the inadequacies of the model to the observations which depends on the model structure and on the parameters defined in the model, $\mathbf{p}$. Additionally, $\varepsilon_{ins}(\cdot, t)$ are the errors associated to instruments, e.g. bias errors, where the notation $(\cdot, t)$ means here that these kind of errors depend of a number of unknown factors not associated to the model structure. Finally, $\varepsilon_{rnd}(\cdot, t)$ stands for random or stochastic errors which usually follows a known statistical distribution function with zero statistical expectation, $\mathsf{E}[\varepsilon_{rnd}(\cdot, t)] = 0$.

Transient responses in OUR measurements are often observed after a sudden increase of a biodegradable substrate in the reacting media, which are not predicted in the context of the IWA activated sludge models. These transients are observed with independence of the system under study or its character, i.e. nitrification or heterotrophic substrate oxidation, and cause an undesirable effect on the accuracy in the determination of the maximum specific biomass growth and in the Monod's saturation constants (μ_{max} and K_S, respectively) and then, in the calibration of the mathematical models. Recently, Vanrolleghem et al. have proposed an interpretation of OUR transients observed in respirometric experiences based on metabolite dynamics for carbon source degradation at an intracellular level [4]. In the same paper, two other hypothesis concerning the non-ideal behaviour of the dissolved oxygen (DO) measuring cell and the mixing regime of the reactors have been checked, concluding that neither of them gives an adequate explanation of the observations. In order to take into account this phenomenon, these authors propose to use an empirical first-order expression to model the observed specific biomass growth, but the proposed equation introduces a new first-order time constant whose physical meaning is not well defined.

The aim of this work is to propose an alternative explanation to the observed transient phenomena in respirometers based on the coupling of some built-in time constants intrinsic to the instrument. The modelling of a hybrid respirometer is reconsidered and all the time constants of the instrument, revised to reduce the systematic errors in OUR determination and parameter estimation. Hence, special attention is paid to time constants such as the oxygen mass transfer coefficient, k_La, and the mean hydraulic residence times of the instrument with its effect on OUR determination. The methodological procedure is based on structural identifiability analysis of the parameters defined in the model under study.

This paper has been structured in three parts. In the first one the different methodologies used for structural identifiability analysis of the models based on local isomorphism transformation are described. The second part is focused on the relevance of the oxygen mass transfer coefficient on OUR determination. The third part reviews the hypothesis used in the determination of OUR using a hybrid respirometer, its connection with transient phenomena and finally, the feasibility of the simultaneous measurement of OUR and DO. The coupling between the different built-in characteristic time-constants of the respirometer as a source of systematic errors of the instrument is considered there.

2. Structural identifiability analysis methodologies

Several methods have been proposed to perform the structural identifiability of dynamical system. The proposed methods for these systems are based on Taylor's series expansion [5,6], or on generating series expansion which amounts to the Laplace transform method for linear state-space models [7–9], methods based on local state space isomorphism theorem (also known as the local isomorphism transformation) [10–12] and finally, to methods derived from differential algebra [13,14]. None of these methodologies are better than others because the success of such analysis depends on the structure itself and the complexity of the model, and then, there are no general rules to apply some methodology to a particular case. For example, Taylor's series method could be easily outlined for complex dynamical systems with a big number of observable state variables, but there are not general methodologies to solve the final set of algebraic equations giving the identifiable parameters. Conversely, the local isomorphism transformation gives a general procedure for the analysis of systems with any level of complexity (together with linear system), but the initial stages of the procedure could give a set of non-linear algebraic equations which are difficult to solve either analytically nor computationally.

Two identifiability methodologies have been used in this work both based on the similarity transformation approach [10]. The first one is an adaptation of this approach to autonomous non-linear rational models proposed by Evans et al. [11]. The second methodology has been recently proposed by Chapman et al. [15,16] as an extension of the local state isomorphism theorem applied for a particular class of non-linear state-space dynamical system. This last one is based on the splitting of the linear and the non-linear part of the state-space model and doing the analysis of both parts separately. We refer the reader to these references for a detailed description of the methods and theirs proofs.

Let us consider the first methodology assuming that our system is described by the following space-state set of ordinary differential equations:

$$\begin{aligned} \dot{\boldsymbol{x}}(t, \boldsymbol{p}) &= \boldsymbol{f}(\boldsymbol{x}(t, \boldsymbol{p}), \boldsymbol{p}), \\ \boldsymbol{x}(0, \boldsymbol{p}) &= \boldsymbol{x}_0(\boldsymbol{p}), \\ \boldsymbol{y}(t, \boldsymbol{p}) &= \boldsymbol{h}(\boldsymbol{x}(t, \boldsymbol{p}), \boldsymbol{p}), \end{aligned} \tag{2}$$

where $\boldsymbol{x}(t, \boldsymbol{p}) \in \mathsf{R}^n$ is the state variable vector, $\dot{\boldsymbol{x}}(t, \boldsymbol{p})$ stands for the time derivative of $\boldsymbol{x}(t, \boldsymbol{p})$ and $\boldsymbol{p} \in \mathsf{R}^m$ is a vector containing the constants and parameters that would be determined from the observable (measurable) vector $\boldsymbol{y}(t, \boldsymbol{p})$. The only restriction applied to functions $\boldsymbol{f}(\cdot, \cdot)$ and $\boldsymbol{h}(\cdot, \cdot)$ is that they are rational in $\boldsymbol{x}$ and $\boldsymbol{p}$. Let's consider here the methodology proposed by Evans et al. [11] for rational uncontrolled systems which is useful in Monod-like models.

Given two parameter vectors $\boldsymbol{p}, \boldsymbol{q} \in \mathsf{R}^m$, we say that they are indistinguishable if they lead to the same input-output behaviour, $\boldsymbol{h}(\boldsymbol{x}(t, \boldsymbol{p}), \boldsymbol{p}) = \boldsymbol{y}(t, \boldsymbol{p}) = \boldsymbol{y}(t, \boldsymbol{q}) = \boldsymbol{h}(\boldsymbol{x}(t, \boldsymbol{q}), \boldsymbol{q})$, which depends only on the structure of the model. If two parameters $\boldsymbol{p}$ and $\boldsymbol{q}$ are indistinguishable in the model structure represented by equation (2), then there exists an unique diffeomorphism $\lambda(\cdot)$ with the following properties:

$$\boldsymbol{H}_{\boldsymbol{p}}(\boldsymbol{\lambda}(\boldsymbol{x}(t, \boldsymbol{p}))) = \boldsymbol{H}_{\boldsymbol{q}}(\boldsymbol{x}(t, \boldsymbol{p})), \tag{3a}$$

$$\boldsymbol{\lambda}(\boldsymbol{x}_0(\boldsymbol{q})) = \boldsymbol{x}_0(\boldsymbol{p}), \tag{3b}$$

$$\boldsymbol{f}(\boldsymbol{\lambda}(\boldsymbol{x}(t, \boldsymbol{q})), \boldsymbol{p}) = \frac{\partial \boldsymbol{\lambda}}{\partial \boldsymbol{x}}(\boldsymbol{x}(t, \boldsymbol{q}))\ \boldsymbol{f}(\boldsymbol{x}(t, \boldsymbol{q}), \boldsymbol{q}), \tag{3c}$$

$$\boldsymbol{h}(\boldsymbol{\lambda}(\boldsymbol{x}(t, \boldsymbol{q})), \boldsymbol{p}) = \boldsymbol{h}(\boldsymbol{x}(t, \boldsymbol{q}), \boldsymbol{q}), \tag{3d}$$

where $\boldsymbol{H}_p(\cdot)$ is a vector field which is used to check the observability rank criterion (ORC) of the system (2) at $\boldsymbol{x}_0(\boldsymbol{p})$, a necessary condition to be hold by the system [10]. This vector is build using a free combination of the observation functions $\boldsymbol{h}(\cdot, \cdot)$ with their successive Lie derivatives along the vector field $\boldsymbol{f}(\cdot, \cdot)$ [11]. Equation (3) have been implemented using a symbolic computation software (Mathematica®, v5.0) to simplify some steps in the identifiability process. The algorithm used in this analysis was:

Step 1. Construction of the vector $\boldsymbol{H}_p(\boldsymbol{x}) = (\mu_1(\boldsymbol{x}, \boldsymbol{p}), \ldots, \mu_n(\boldsymbol{x}, \boldsymbol{p}))^{\mathsf{T}}$, where $\mu_i(\boldsymbol{x}, \boldsymbol{p})$ are functions derived from the components of $\boldsymbol{h}(\cdot, \cdot)$ and $\boldsymbol{f}(\cdot, \cdot)$.

Step 2. Check the ORC of the system calculating the Jacobian of $\boldsymbol{H}_p(\boldsymbol{x})$; if $\mathrm{Det}\left(\frac{\partial \boldsymbol{H}_p(\boldsymbol{x})}{\partial \boldsymbol{x}}\right)_{\boldsymbol{x}0} \neq 0$, then the system satisfies the ORC, otherwise return to step 1.

Step 3. Calculation of $\lambda(\cdot)$ by inversion of equation (3a): $\lambda(\boldsymbol{x}(t, \boldsymbol{p})) = \boldsymbol{H}_p^{-1}(\boldsymbol{H}_q(\boldsymbol{x}(t, \boldsymbol{p})))$.

Step 4. Verification of the relation between the vector parameters $\boldsymbol{p}$ and $\boldsymbol{q}$ using equation (3c).

Step 5. Additional relations between $\boldsymbol{p}$ and $\boldsymbol{q}$ are derived using equations (3b) or (3d).

Since $\boldsymbol{h}(\cdot)$ and $\boldsymbol{f}(\cdot,\cdot)$ are rational functions, the solution of equation (3c) leads to a non-linear polynomial equation in $\boldsymbol{x}(t,\cdot)$ from which the relations involving $\boldsymbol{p}$ and $\boldsymbol{q}$ are obtained equating all their coefficients to zero. Let us apply the algorithm to a simple case, e.g. monosubstrate consumption with Monod kinetics in extant conditions. After equation (2), this system could be written as:

$$\begin{aligned} \dot{x}_1 &= -\frac{p_1}{p_2}\frac{x_1}{p_3+x_1}p_4, \\ x_1(0) &= p_5, \\ y(t) &= \frac{1-p_2}{p_2}p_1\frac{x_1}{p_3+x_1}p_4, \end{aligned} \tag{4}$$

where $p_1 = \mu_{\max}$, $p_2 = Y$, $p_3 = K_S$, $p_4 = X_0$, and $p_5 = S_0$. The state-variable x_1 stands in the model for the substrate concentration, S, and the observable function, $y(t)$, stands for the exogenous OUR. Applying the algorithm described above, we have:

Step 1. Since the observable function in system (4) is unique, our first guess for $\boldsymbol{H}_p(\boldsymbol{x},\boldsymbol{p})$ is:

$$H_p(x,p) = \frac{1-p_2}{p_2}p_1\frac{x_1}{p_3+x_1}p_4. \tag{5}$$

Step 2. Knowing that the yield is bounded, $p_2 < 1$, then the system satisfies the ORC because,

$$\left.\frac{\partial H_p(x,p)}{\partial x_1}\right|_{x_1=p_5} = \frac{1-p_2}{p_2}\,\frac{p_1\ p_3\ p_4}{(p_3+p_5)^2} \neq 0 \quad \forall \boldsymbol{p} > 0. \tag{6}$$

Step 3. From equation (3a), $\lambda(\boldsymbol{x}(t,\boldsymbol{q})) = H_{\boldsymbol{p}}^{-1}\left(H_{\boldsymbol{q}}(\boldsymbol{x}(t,\boldsymbol{p}))\right)$, then in our case:

$$\lambda_1 = \frac{-q_1\ p_2(1-q_2)\ p_3\ q_4\ x_1}{q_1\ p_2(1-q_2)\ q_4\ x_1 - p_1\ q_2(1-p_2)\ p_4\ (q_3+x_1)}. \tag{7}$$

Step 4. Equation (3c) gives the polynomial:

$$A(\boldsymbol{p},\boldsymbol{q})\ x_1^3 + B(\boldsymbol{p},\boldsymbol{q})\ x_1^2 + C(\boldsymbol{p},\boldsymbol{q})\ x_1 + D(\boldsymbol{p},\boldsymbol{q}) = 0,$$

where

$$A(\boldsymbol{p},\boldsymbol{q}) = q_1(1-q_2)q_4\left[-p_1q_2(1-p_2)p_4 + q_1p_2(1-q_2)q_4\right]^2, \tag{8a}$$

$$\begin{aligned} B(\boldsymbol{p},\boldsymbol{q}) = -2p_1(1-p_2)p_4q_1(1-q_2)q_2q_3q_4\left[-p_1q_2(1-p_2)p_4\right. \\ \left. + q_1p_2(1-q_2)q_4\right], \end{aligned} \tag{8b}$$

$$C(\boldsymbol{p},\boldsymbol{q}) = -p_1(1-p_2)^2 p_4 q_1 (1-q_2) q_2 q_3 q_4 \left[-p_1 p_4 q_2 q_3 + q_1 q_4 p_2 p_3\right], \quad (8c)$$

$$D(\boldsymbol{p},\boldsymbol{q}) = 0. \quad (8d)$$

Since x_1 is not equal to zero, the polynomial might be zero if and only if $A(\boldsymbol{p},\boldsymbol{q}) = B(\boldsymbol{p},\boldsymbol{q}) = C(\boldsymbol{p},\boldsymbol{q}) = D(\boldsymbol{p},\boldsymbol{q}) = 0$. Equating to zero the terms in brackets, we have:

$$\frac{p_1 p_4}{p_2 p_3} = \frac{q_1 q_4}{q_2 q_3}, \quad (9)$$

$$\frac{1-p_2}{p_2} p_1 p_4 = \frac{1-q_2}{q_2} q_1 q_4. \quad (10)$$

Step 5. Considering the precedent expressions and (3b), the following additional relation is deduced:

$$\frac{p_3}{p_5} = \frac{q_3}{q_5}. \quad (11)$$

In conclusion, the model defined by equation (3) is unidentifiable with three parameter groups, namely (9)–(11) which correspond, respectively, to:

$$\frac{\mu_{\max} X_0}{Y\ K_S}, \qquad \frac{1-Y}{Y}\mu_{\max} X_0, \qquad \frac{K_S}{S_0}. \quad (12)$$

After some algebraic manipulations, it can be demonstrated that these groups are equivalent to those obtained using the Talyor's series method for structural identifiability of model (4) (e.g. see equation (4.146) in [3]).

The second methodology for structural identifiability analysis used in this work is useful for a particular kind of compartmental models which are common in chemical processes. Let consider that the process under study could be described by the non-linear state-space model of the form:

$$\dot{\mathbf{x}}(t,\mathbf{p}) = \mathbf{A}(\mathbf{p})\ \mathbf{x}(t,\mathbf{p}) + \mathbf{B}(\mathbf{p})\ \mathbf{u}(t) + \sum_{i=1}^{s} f_{\mathbf{i}}\left(\mathbf{x}\left(t,\mathbf{p}\right),\mathbf{p}\right)\ \nu_{\mathbf{i}}(\mathbf{p}), \quad (13a)$$

$$\mathbf{z}(t,\mathbf{p}) = \mathbf{C}(\mathbf{p})\ \mathbf{x}(t,\mathbf{p}), \quad (13b)$$

$$\mathbf{x}(0,\mathbf{p}) = \mathbf{0} \quad (13c)$$

with the additional properties:

$$\begin{aligned} \boldsymbol{f}_i(0, \mathbf{p}) &= 0, \\ \frac{\partial \boldsymbol{f}_i}{\partial \mathbf{x}_i}(0, \mathbf{p}) &= 0, \end{aligned} \tag{14}$$

where $\mathbf{x}(t, \mathbf{p}) \in \mathsf{R}^n$ is the state variable vector, $\dot{\mathbf{x}}(t, \mathbf{p})$ stands for the time derivative of $\mathbf{x}(t, \mathbf{p})$ and $\mathbf{p}$ is a vector containing the constants and parameters that would be determined from the observable (measurable) vector $\mathbf{z}(t, \mathbf{p})$. Notice that the observable magnitudes, $\mathbf{z}(t, \mathbf{p})$, are linearly related with the state variables, $\mathbf{x}(t, \mathbf{p})$, but could be non-linearly related with the parameters of the model, $\mathbf{p}$, through the observation matrix $\mathbf{C}(\mathbf{p})$. The input vector, $\mathbf{u}(t) \in \mathsf{R}^r$, is also considered bounded and measurable and represents the perturbation applied to the system from the outwards of its bounds. On the other hand, $\boldsymbol{f}_i(\mathbf{x}(t, \mathbf{p}), \mathbf{p}), i = 1, \ldots, s$ are the non-linear functions in $\mathbf{x}$ and $\mathbf{p}$ of the equations system. Finally, $\mathbf{A}(\mathbf{p})$, $\mathbf{B}(\mathbf{p})$, $\mathbf{C}(\mathbf{p})$ and $\boldsymbol{v}_i(\mathbf{p})$ are matrices which define the system and describe the relationship between the state vector, $\mathbf{x}(t, \mathbf{p})$, the perturbation applied to the system, $\mathbf{u}(t)$, and the physically observed response, $\mathbf{z}(t, \mathbf{p})$. Thus, after equations (13) and (14) the system is described by at set of first-order ODE's that have a linear and a non-linear component. Moreover, the additional conditions (14) ensure that the system is initially in a stationary state and there is not contribution of the non-linear part to the linear one.

Two parameters, $\mathbf{p}$ and $\mathbf{q}$, are indistinguishable in the model structure represented by equation (13) if there exists a function $\lambda(\mathbf{x}) = \mathbf{T}\mathbf{x} + \mu(\mathbf{x})$, with $\mathbf{T} \in \mathsf{R}^{n \times n}$ and $\mu(\mathbf{x}) \in \mathsf{R}^n$ where the linear part holds:

$$\mathbf{C}(\mathbf{q})\ \mathbf{T} = \mathbf{C}(\mathbf{p}), \tag{15a}$$

$$\mathbf{B}(\mathbf{q}) = \mathbf{T}\ \mathbf{B}(\mathbf{p}), \tag{15b}$$

$$\mathbf{A}(\mathbf{q})\ \mathbf{T} = \mathbf{T}\ \mathbf{A}(\mathbf{p}) \tag{15c}$$

together with the non-linear equations:

$$\mathbf{C}(\mathbf{q}) \cdot \boldsymbol{\mu}(\mathbf{x}) = \mathbf{0}, \tag{16a}$$

$$\frac{\partial \boldsymbol{\mu}}{\partial \mathbf{x}}(\mathbf{x}) \cdot \mathbf{B}(\mathbf{p}) = \mathbf{0}, \tag{16b}$$

$$\begin{aligned} \mathbf{A}(\mathbf{q}) \cdot \boldsymbol{\mu}(\mathbf{x}) + \sum_i f_i(\mathbf{x}(\mathbf{q}), \mathbf{q}) = \frac{\partial \boldsymbol{\mu}}{\partial \mathbf{x}}(\mathbf{x}) \cdot \mathbf{A}(\mathbf{p}) \cdot \mathbf{x} \\ + \left(\mathbf{T} + \frac{\partial \boldsymbol{\mu}}{\partial \mathbf{x}}(\mathbf{x})\right) \sum_i f_i(\mathbf{x}(\mathbf{q}), \mathbf{q}). \end{aligned} \tag{16c}$$

The system is structurally globally identifiable if $\mathbf{T} = \mathbf{I}$ and $\boldsymbol{\mu}(\mathbf{x}) = \mathbf{0}$, where $\mathbf{I}$ is the identity matrix.

The advantage of this procedure is that if the analysis of the linear part of the model (equation (15)) gives the parameters which are globally identifiables, the analysis of the non-linear part of this theorem (equation (16)), which usually is much more complicated, is not needed. Moreover, another advantage of this method is that equation (15) could be solved simultaneously using computer algebra as is described elsewhere [15,17]. Nevertheless, the disadvantage of this method is that it is limited to models described by equation (13) subject to restrictions given by equation (14).

In the next section, it will be used the methodology proposed by Evans et al. [11] to analyse the simplest model for respirometry accounting for the oxygen mass transfer to water. Afterwards, it will be used the method proposed by Chapman et al. [15] to analyse the model describing the hybrid respirometer.

3. Models accounting for oxygen mass transfer

As it was suggested at the introduction, the knowledge of the built-in time constants of a hybrid respirometer is capital to control or reduce the systematic errors in the OUR or biokinetic parameters determination. By built-in time constants should be understood the constants associated to the instrument arisen from dynamic physical processes, e.g. mass transfer processes. These constants could be coupled each other with chemical rate constants which makes complex the understanding of the experimental data.

In order to state the problem, let us consider a hybrid respirometer such as described in [18] (see figure 1). Three time constants could be defined in such system: the oxygen mass transfer coefficient and the two hydraulic retention times associated to water flow between the aerobic and the respiration chambers. Let us analyse before the simplest case of the instrument, where there is no flow between both chambers, i.e. $Q = 0$, and the oxygen concentration measurement is carried out at the aerobic chamber, V_1. In this situation, a model accounting for the oxygen mass transfer in combination with the biochemical processes should be considered. Because the magnitude OUR is derived from DO measurements, the structural identifiability analysis of the model could be done considering each one separately or both together. Thus, these two magnitudes lead to three different cases to analyse which will be described in detail later.

The model previously analysed and described by equation (4) does not include the parameters that we would like to measure, i.e. the mass transfer coefficient, $k_L a$, and the steady state oxygen saturation concentration, C^*. Thus, let us write the system of ODE in extant conditions considering additionally the oxygen mass transfer. Also, it might be considered that the OUR is known with independence of DO measurements, coming back at this point further. Then,

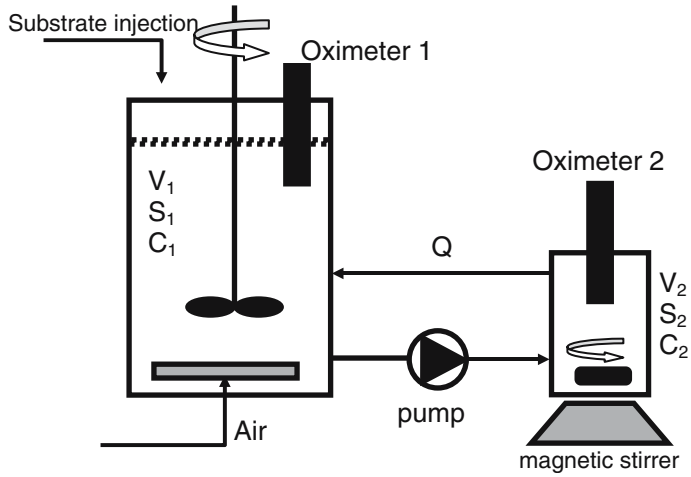

Figure 1. Hybrid respirometer scheme. The aerobic and the respiration chamber are connected with a pump giving a constant flow rate, Q. Both reactors are considered ideal CSTR. Usually, the DO is continuously measured along each experiment with the two oximeters, while the OUR is derived after equation (42b). The substrate injection has been considered as an input in the model given by equation (43).

under these circumstances, we have:

$$\dot{S} = -\frac{\mu_{\max}}{Y} X_0 \frac{S}{K_S + S}, \quad S(0) = S_0, \tag{17}$$

$$\dot{C} = k_L a \left(C^* - C\right) - \frac{1 - Y}{Y} \mu_{\max} X_0 \frac{S}{K_S + S}, \quad C(0) = C_0, \tag{18}$$

$$OUR_{\text{exo}} = R_{\text{exo}} = \frac{1 - Y}{Y} \mu_{\max} X_0 \frac{S}{K_S + S}, \tag{19}$$

where S is the substrate concentration, C the DO concentration and R_{exo} the exogenous OUR. Assuming this model, the OUR is calculated from experimental measurements with:

$$R_{\text{exo}} = k_L a \left(C^* - C\right) - \dot{C}. \tag{20}$$

Hence, the systematic errors associated to this magnitude depend on the oxygen mass transfer coefficient, the oxygen saturation concentration, on the systematic errors associated to DO measurements and finally, on the numerical procedure used to calculate the oxygen derivative. Let us demonstrate here the identifiability of $k_L a$ and C^* considering that the OUR and the DO are independently known whichever the experimental technique was used for its determination and considering that they are free of systematic errors.

After the notation given by equation (2), the systems (17)–(19) could be written as:

$$\dot{x}_1 = -\frac{p_1}{p_2} p_4 \frac{x_1}{p_3 + x_1}, \quad x_1(0) = p_5, \tag{21}$$

$$\dot{x}_2 = p_6(p_7 - x_2) - \frac{1 - p_2}{p_2} p_1 p_4 \frac{x_1}{p_3 + x_1}, \quad x_2(0) = p_8, \tag{22}$$

where the state-variables x_1 and x_2 are $S(t)$, and $C(t)$, respectively. The parameters are $p_1 = \mu_{\max}$, $p_2 = Y$, $p_3 = K_S$, $p_4 = X_0$, $p_5 = S_0$, $p_6 = k_L a$, $p_7 = C^*$ and $p_8 = C_0$. At this point three cases could be analysed considering such as many possible ways to define the observable vector $\boldsymbol{h}(\boldsymbol{x}, \boldsymbol{p})$.

Case I Only OUR. In this case, only the OUR is the observable magnitude of the system. Let us consider the first step of the algorithm. After equation (2) we have:

$$y(t) = h(\boldsymbol{x}, \boldsymbol{p}) = \frac{1 - p_2}{p_2} p_1 p_4 \frac{x_1}{p_3 + x_1}, \tag{23}$$

$$H_{\boldsymbol{p}}(\boldsymbol{x}) = \left(\frac{p_1(1-p_2)p_4}{p_2} \;\; \frac{x_1}{p_3+x_1} \;\; -\frac{p_1^2(1-p_2)p_3p_4^2}{p_2^2} \;\; \frac{x_1}{(p_3+x_1)^3} \right)^{\mathsf{T}}. \tag{24}$$

The second element in vector (24) is the first Lie derivative of the equation (23) along equations (21) and (22). Note that none of the elements is a function of x_2. Consequently, the rank of the Jacobian matrix of the vector $\boldsymbol{H}_p(\boldsymbol{x})$ will always be less than the rank of the model because the derivative terms respect x_2 are always zero. Therefore, the models (21) and (22) **does not satisfy the observable rank condition** when the observable function is just given by equation (23) and then, the model is not observable.

Case II Only DO. Considering that the DO is the single observable magnitude of the model, we have:

$$y(t) = h(\boldsymbol{x}, \boldsymbol{p}) = x_2, \tag{25}$$

$$H_{\boldsymbol{p}}(\boldsymbol{x}) = \left(x_2 \;\; \frac{p_1(1-p_2)p_4}{p_2} \;\; \frac{x_1}{p_3+x_1} \right)^{\mathsf{T}}. \tag{26}$$

Notice that the dimension of the vector $\boldsymbol{H}_p(\boldsymbol{x})$ must be equal to the number of state variables in the model, and that it is built using first the observable functions and their Lie derivatives afterwards. It can be demonstrated that the determinant of the Jacobian matrix of (26) is not null at $\boldsymbol{x}(0)$, and thus, the model satisfies the ORC in these conditions. Hence, applying steps 3 and 4 of the algorithm, a non-linear polynomial in x_1 and x_2 with 16 coefficients is obtained

(not shown here for brevity) which after their analysis, the following parameter groups could be identified:

$$\frac{\mu_{\max} X_0}{Y\ K_S}, \qquad \frac{1-Y}{Y}\mu_{\max} X_0, \quad k_L a, \quad C^*. \tag{27}$$

Additionally, after applying the property (3d) the following groups related with the initial conditions of equations (17) and (18) also hold:

$$\frac{K_S}{S_0}, \quad C_0. \tag{28}$$

After this analysis it can be concluded that the dissolved oxygen data are just enough to determine the parameter groups given by equations (27) and (28), which in turn are the same that the obtained in the precedent model plus the parameters related with the oxygen transfer. Thus, the manipulation of the raw data, i.e. the DO readings to calculate the measure of the OUR, could not be essential in the determination of biokinetic parameters. After all, the same parameter groups are identifiable using the easiest of the observable magnitudes.

Case III. OUR + DO. In this case, the simultaneous measurement of the OD and the OUR is considered. Thus, the observable vector is given by:

$$y(t) = \boldsymbol{h}(\boldsymbol{x}, \boldsymbol{p}) = \left(x_2 \ \frac{p_1(1-p_2)p_4}{p_2} \ \frac{x_1}{p_3+x_1} \right)^T \tag{29}$$

from which we should build the vector $\boldsymbol{H}_p(\boldsymbol{x})$. Our first guess is to equal both functions because equation (29) form the basis set from which the vector $\boldsymbol{H}_p(\boldsymbol{x})$ is built. Notice that equation (26) is the same that equation (29) and then, all the conclusions deduced in the precedent case about the structural identifiability of the model are also applicable to this case. Hence, equations (27) and (28) also hold when the DO and OUR are simultaneously measured.

After the analysis, it is concluded that the DO measurement is compulsory in order to obtain the mass transfer coefficient in a biological reactor. This conclusion, that could be understood intuitively, has been demonstrated here conclusively. In addition, it could also be demonstrated that if the observation function, e.g. equation (23), is considered with an endogenous respiration term, the final conclusion in the three cases do not change. It can be demonstrated that in cases II and III the endogenous respiration parameter could also be identifiable in the model when the DO is used as an observable function.

Finally, let us consider a more general model that the described by equations (21) and (22), where the biomass growth is considered and the observation

functions are the OUR and DO simultaneously. Thus, the model is defined by:

$$\dot{S} = -\frac{\mu_{\max}}{Y}\frac{S}{K_S + S}X, \quad S(0) = S_0, \tag{30}$$

$$\dot{X} = \mu_{\max}\frac{S}{K_S + S}X - b_H X, \quad X(0) = X_0, \tag{31}$$

$$\dot{C} = k_L a\left(C^* - C\right) - \frac{1 - Y}{Y}\mu_{\max}\frac{S}{K_S + S}X, \quad C(0) = C_0, \tag{32}$$

where b_H is the endogenous rate constant. After the analysis of the precedent model, it has been noticed that if the observation vector, $\boldsymbol{h}(\boldsymbol{x}, \boldsymbol{p})$, is built with the raw state variables of the model, the algorithm could be more efficiently applied from a computational point of view. Since the OUR is initially considered as a valid state variable and is not explicitly defined in the precedent model, let us insert a new differential equation after the definition of the exogenous respiration rate:

$$R_{\text{exo}} = \frac{1 - Y}{Y}\mu_{\max}\frac{S}{K_S + S}X, \tag{33}$$

$$\begin{aligned}\dot{R}_{\text{exo}} &= \left(\frac{\partial R_{\text{exo}}}{\partial S}\right)\dot{S} + \left(\frac{\partial R_{\text{exo}}}{\partial X}\right)\dot{X} \\ &= \left[\frac{\mu_{\max}(Y\ S\ (K_S + S) - K_S X}{Y(K_S + S)^2} - b_H\right]\ R_{\text{exo}}.\end{aligned} \tag{34}$$

After rearranging equations (30)–(32) and (34), the model could be rewritten as:

$$\dot{x}_1 = -\frac{1}{1 - p_2}x_3, \tag{35a}$$

$$\dot{x}_2 = \frac{p_2}{1 - p_2}x_3 - p_4\ x_2, \tag{35b}$$

$$\dot{x}_3 = \left(\frac{p_1\ (p_2\ x_1\ (p_3 + x_1) - p_3\ x_2)}{p_2(p_3 + x_1)^2} - p_4\right)x_3, \tag{35c}$$

$$\dot{x}_4 = p_5(p_6 - x_4) - x_3 \tag{35d}$$

with the following initial values vector:

$$\boldsymbol{x}(0) = \left(p_7\ p_8\ \frac{1 - p_2}{p_2}p_1\ \frac{p_7}{p_3 + p_7}p_8\ p_9\right)^{\mathsf{T}}, \tag{36}$$

where $p_1 = \mu_{\max}$, $p_2 = Y$, $p_3 = K_S$, $p_4 = b_H$, $p_5 = k_L a$, $p_6 = C^*$, $p_7 = S_0$, $p_8 = X_0$ and $p_9 = C_0$. Remark that equation (35) and the initial conditions (36)

are equivalent to equations (30)–(32) and (34) with $x_1 = S(t)$, $x_2 = X(t)$, $x_3 = R_{\text{exo}}(t)$ and $x_4 = C(t)$, respectively. The observation vector is given by its simplest case, that is, the OUR and the DO:

$$\boldsymbol{h}(\boldsymbol{x}, \boldsymbol{p}) = \begin{pmatrix} x_3 & x_4 \end{pmatrix}^{\mathsf{T}}. \tag{37}$$

The vector field $\boldsymbol{H}_p(\boldsymbol{x})$ is built using equation (37) and its successive Lie derivatives. Let $\mathcal{L}_f \boldsymbol{h}(\boldsymbol{x})$ the Lie derivative of $\boldsymbol{h}$, the observable vector, along the vector field $\boldsymbol{f}$, the right hand terms of equation (35). Considering the first step in the algorithm described above, let $\mu_1(\boldsymbol{x}, \boldsymbol{p}) = h_1(\boldsymbol{x}, \boldsymbol{p}) = x_3$ and $\mu_2(\boldsymbol{x}, \boldsymbol{p}) = h_2(\boldsymbol{x}, \boldsymbol{p}) = x_4$ and define:

$$\boldsymbol{H}_{\boldsymbol{p}}(\boldsymbol{x}, \boldsymbol{p}) = \begin{pmatrix} \mu_1 & \mu_2 & \mathcal{L}_f \mu_1 & \mathcal{L}_f(\mathcal{L}_f \mu_1) \end{pmatrix}^{\mathsf{T}}. \tag{38}$$

The Jacobian matrix of this vector has full rank, and then, the model (35) satisfies the ORC at $\boldsymbol{x}(0)$. After the inversion of equation (38) and applying (3c), four non-linear polynomials in $\boldsymbol{x}$ are obtained which must be equal to zero for all $\boldsymbol{x}$. One of them satisfies equation (3c) automatically and no information about the identifiable parameter groups could be derived from it. A second one, gives the following equation:

$$p_5 p_6 - q_5 q_6 + (q_5 - p_5)\, x_4 = 0. \tag{39}$$

Because the elements $\boldsymbol{p}$ and $\boldsymbol{x}$ are all of them positive magnitudes, equation (39) is satisfied if and only if $p_5 = q_5$ and $p_6 = q_6$. Hence, the identifyability of $k_L a$ and C^* has been proved when OUR and DO define the observation vector (37) of the models (35) and (36). The two remaining polynomials are extremely large summing up to 442 coefficients, but by using some symbolic algebra, they can be easily reduced. Considering (39) and the reduced polynomials, it is concluded that the following parameter groups are indentifiables in the model given by equations (35)–(37):

$$k_L a, \quad C^*, \quad \mu_{\max}, \quad b_H, \quad (1 - Y) K_{\text{S}}. \tag{40}$$

Additionally, applying equation (3.b) the following also holds:

$$\frac{K_{\text{S}}}{S_0}, \quad \frac{Y\ K_{\text{S}}}{X_0}, \quad \frac{1 - Y}{Y} \frac{S_0\ X_0}{K_{\text{S}} + S_0}, \quad C_0. \tag{41}$$

Notice that if the yield, Y, is known, the system becomes *globally structurally identifiable* because its input-output structure is unique with a given set of parameters.

In summary, the simultaneous knowledge of the DO concentration and the OUR allows the simultaneous determination of the oxygen mass transfer parameters and the biokinetic parameters. After rearranging the Monod model

with biomass growth (see equations (30)–(32) and (34)), it has also been demonstrated that the knowledge of the system could be even better than when extant conditions are assumed. All the precedent demonstrations have been carried out considering that the OUR is a known magnitude whichever technique or methodologies were used for its determination. This assumption was just formulated to do the structural identifiability analysis of the models considering different observable functions, but it remains as an uncorroborated hypothesis. Thus, let us consider in the next section the feasibility of the simultaneous determination of the DO and the OUR in the hybrid respirometry context.

4. Structural identifiability analysis of the hybrid respirometer model

The problem now to be treated, not only should be solved considering a biokinetic model but also, a precise description of the instrumentation to be used. Let us consider an hybrid respirometer such as described in [18] working in a LFF+LSF configuration (see figure 1 with $Q \neq 0$). Assuming two control volumes associated to each reactor, the set of ODE's describing the behaviour of this system in extant conditions is given by:

$$\dot{C}_1 = \tau_1^{-1}(C_2 - C_1) + k_L a(C^* - C_1) - R_1, C_1(0) = C_0, \tag{42a}$$

$$\dot{C}_2 = \tau_2^{-1}(C_1 - C_2) - R_2, \quad C_2(0) = C_0, \tag{42b}$$

$$\dot{S}_1 = \tau_1^{-1}(S_2 - S_1) - \frac{1}{1-Y}R_1, \quad S_1(0) = S_0, \tag{42c}$$

$$\dot{S}_2 = \tau_2^{-1}(S_1 - S_2) - \frac{1}{1-Y}R_2, \quad S_2(0) = 0, \tag{42d}$$

where the indexes stand for the aerobic reactor and the respiration chamber, respectively. Both reactors are characterized by its mean hydraulic residence time, τ_i. Additionally, the OURs in the reactors, R_i, are considered different in magnitude because the difference between the substrate concentration in both chambers. The usual way to obtain the OUR with the respirometer is working out R_2 from equation (42b) and considering that this value does not differ significantly from R_1. The problem is, in our opinion, that although R_2 could be considered as the true OUR value calculated for the biological system under study, it is not possible to apply the initial conditions given by equation (42c) or even assume that the OUR could be assigned to a system such as given by equations (17)–(19) basically because $R_1 \neq R_2 \neq R_{exo}$. This is particularly true at the beginning of the experiments because the initial substrate concentration in both reactors differ significantly (see equations (42c) and (42d)).

Since under these circumstances R_2 cannot be considered as a state variable of the system (42), it cannot be used for the structural identifiability analysis of the model. Then, let us analyse the identifiability of the system from their true accessible state variables, i.e. the oxygen concentrations C_1 and C_2.

The model structure itself suggests to try the second methodology for structural identifiability described in section 2. Consequently, the system (42) should be rewritten satisfying the conditions imposed by equations (13) and (14) and considering a particular biokinetic model. Before this, let us think about how a respirometric experiment is carried out. Once the reactors are filled and the biomass set in extant conditions, an injection of substrate in the aerobic reactor is done while the DO electrodes are continuously acquiring data. In this context, the substrate injection could be described more accurately such as a substrate pulse of duration δ or like an additional flow input in the reactor working discontinuously (see figure 1).

Considering this experimental procedure and equations (13) and (14), let us rewrite the system (42) with the following additional conditions:

1. The substrate consumption is described by a Monod's kinetics.
2. The system is initially at rest and the substrate concentration is null in both reactors, $S_1(0) = S_2(0) = 0$.
3. The substrate injected in the respirometer is easily biodegradable with a known COD. This process is considered finite and is carried out in a time δ small enough but not null.
4. The endogenous respiration in the model is negligible compared with the exogenous one.
5. The oxygen concentration before the substrate injection, has reached its saturation value, $C_0 = C^*$.
6. The temperature is constant.

Under these circumstances, the system could be written as follow:

$$\dot{x}_1 = p_1 (x_2 - x_1) - p_3\, x_1 + \frac{1 - p_5}{p_5}\frac{p_6 p_7}{p_4 p_8} x_3 - \frac{1 - p_5}{p_5}\frac{p_6 p_7}{p_4 p_8}\frac{x_3^2}{p_8 + x_3}, \quad x_1(0) = 0, \tag{43a}$$

$$\dot{x}_2 = p_2 (x_1 - x_2) + \frac{1 - p_5}{p_5}\frac{p_6 p_7}{p_4 p_8} x_4 - \frac{1 - p_5}{p_5}\frac{p_6 p_7}{p_4 p_8}\frac{x_4^2}{p_8 + x_4}, \quad x_2(0) = 0, \tag{43b}$$

$$\dot{x}_3 = p_1 (x_4 - x_3) + N \cdot U(t) - \frac{p_6 p_7}{p_4 p_8} x_3 + \frac{p_6 p_7}{p_4 p_8}\frac{x_3^2}{p_8 + x_3}, \quad x_3(0) = 0, \tag{43c}$$

$$\dot{x}_4 = p_2 (x_3 - x_4) - \frac{p_6 p_7}{p_4 p_8} x_4 + \frac{p_6 p_7}{p_4 p_8}\frac{x_4^2}{p_8 + x_4}, \quad x_4(0) = 0, \tag{43d}$$

where x_1 and x_2 are the state variables related to the DO concentration through $x_1 = 1 - C_1/C^*$ and $x_2 = 1 - C_2/C^*$, while x_3 and x_4 are the substrate

concentrations as were previously defined in equations (42c) and (42d). Notice that all the initial conditions are set to zero and that the substrate injection is included through the perturbation function $U(t)$. The parameters in the model are $p_1 = Q\Big/V_1 = \tau_1^{-1}$, $p_2 = Q\Big/V_2 = \tau_2^{-1}$, $p_3 = k_L a$, $p_4 = C^*$, $p_5 = Y$, $p_6 = \mu_{\max}$, $p_7 = X_0$ and $p_8 = K_S$. The constant N and the injection-function $U(t)$ in (43c) are defined by:

$$N = \frac{n_0}{V_1 \cdot \delta}, \tag{44}$$

$$U(t) = H(t) - H(t-\delta), \tag{45}$$

where n_0 is the total substrate COD injected in the respirometer, δ the injection-time and $H(t)$ is the Heaviside unitary step function. Finally, comparing equation (43) with equations (13) and (14) we have:

$$\boldsymbol{A}(\boldsymbol{p}) = \begin{pmatrix} -(p_1+p_3) & p_1 & \frac{1-p_5}{p_5}\frac{p_6 p_7}{p_4 p_8} & 0 \\ p_2 & -p_2 & 0 & \frac{1-p_5}{p_5}\frac{p_6 p_7}{p_4 p_8} \\ 0 & 0 & -p_1 - \frac{p_6 p_7}{p_4 p_8} & p_1 \\ 0 & 0 & p_2 & -p_2 - \frac{p_6 p_7}{p_4 p_8} \end{pmatrix}, \tag{46}$$

$$\boldsymbol{B}(\boldsymbol{p}) = \begin{pmatrix} 0 & 0 & N & 0 \end{pmatrix}^{\mathsf{T}}. \tag{47}$$

Since the observable magnitudes of our system are the oxygen concentration in both chambers of the respirometer, three different observation matrices could be defined:

$$\boldsymbol{C}_{\mathrm{I}}(\boldsymbol{p}) = \begin{pmatrix} 1 & 0 & 0 & 0 \end{pmatrix}, \tag{48a}$$

$$\boldsymbol{C}_{\mathrm{II}}(\boldsymbol{p}) = \begin{pmatrix} 0 & 1 & 0 & 0 \end{pmatrix}, \tag{48b}$$

$$\boldsymbol{C}_{\mathrm{III}}(\boldsymbol{p}) = \begin{pmatrix} 1 & 0 & 0 & 0 \\ 0 & 1 & 0 & 0 \end{pmatrix}. \tag{48c}$$

The first two matrices correspond to single oxygen concentration measurements in the aerobic and respiration chamber, respectively, while the third matrix represents the simultaneous measurement of both state variables in a single experiment.

The matrix (46) could be simplified considering that p_2 and p_1 are related through a known constant, $K = V_1/V_2$, which relates the volume between the aerobic and the respiration chambers of the respirometer.

$$\boldsymbol{A}(\boldsymbol{p}) = \begin{pmatrix} -(p_1 + p_3) & p_1 & \frac{1-p_5}{p_5}\frac{p_6 p_7}{p_4 p_8} & 0 \\ K\ p_1 & -K\ p_1 & 0 & \frac{1-p_5}{p_5}\frac{p_6 p_7}{p_4 p_8} \\ 0 & 0 & -p_1 - \frac{p_6 p_7}{p_4 p_8} & p_1 \\ 0 & 0 & K\ p_1 & -K\ p_1 - \frac{p_6 p_7}{p_4 p_8} \end{pmatrix}. \tag{49}$$

Solving equation (15) for $\boldsymbol{T}$ with any of the matrices defined by (48), we find that:

$$\boldsymbol{T} = \begin{pmatrix} 1\,0\,0\,0 \\ 0\,1\,0\,0 \\ 0\,0\,1\,0 \\ 0\,0\,0\,1 \end{pmatrix} \tag{50}$$

together with:

$$p_1 = q_1, \qquad p_3 = q_3, \qquad \frac{p_4}{1-p_5} = \frac{q_4}{1-q_5}, \qquad \frac{p_6 p_7}{p_5 p_8} = \frac{q_6 q_7}{q_5 q_8}. \tag{51}$$

Thus, the parameter groups identifiable in the model are:

$$\tau_1, \quad k_L a, \quad \frac{C^*}{1-Y}, \quad \frac{\mu_{\max} X_0}{Y\ K_S}. \tag{52}$$

Since C^* is known because it is equal to the initial saturation oxygen concentration (see condition no.5 above), the heterotrophic biomass yield, Y, is identifiable in the model. Additionally, since τ_1 is identifiable and K is known, τ_2 could be derived from these magnitudes. And finally, since $k_L a$ is identifiable too, the OURs R_1 and R_2 can be derived from model (42) if the last group of parameters in (52) is known. Notice that although the biomass yield could be identified using this model, the constants $\mu_{\max}$, K_S and X_0, cannot be uncoupled to each other.

Figure 2 shows simulations of the model (42) with a typical set of biokinetic parameters. The DO and the substrate profiles in the two chambers of the respirometer are shown in figure 2a and b, respectively. Remark the discrepancy between the substrate concentrations at the initial stages of the simulation. This difference is in the origin of the transient phenomena observed in the OUR measurements. From DO data (figure 2a), the OUR at the respiration chamber is calculated using equation (42b) and plotted in figure 2c. Notice a small transient at initial stages of the substrate injection which is not predicted by the Monod's model but by equation (42). The slope of this curve at the origin could be obtained from both models showing a huge discrepancy between them. From the

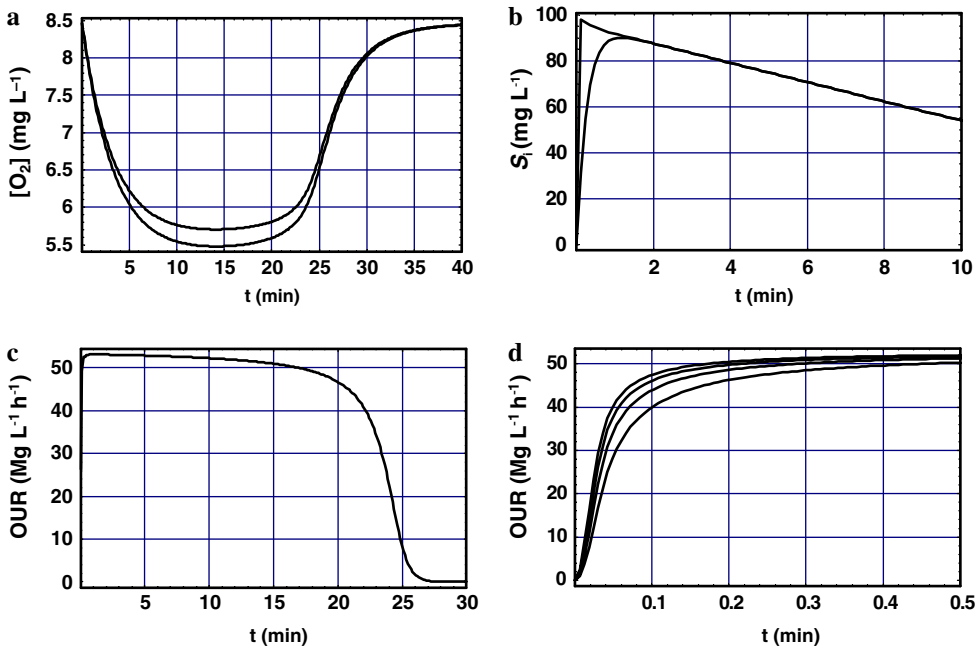

Figure 2. Numerical simulation of model (43) showing the OUR transient resulting from the coupling between the biological kinetics and the reactor hydrodynamics. The parameters selected for the simulation are typical for an easily biodegradable substrate $Q = 48\,\mathrm{L/h}$; $V_1 = 5\,\mathrm{L}$; $V_2 = 212\,\mathrm{mL}$; $k_La = 19.4\,\mathrm{h}^{-1}$; $C* = 8.46\,\mathrm{mg/L}$; $Y = 0.79$; $\mu_{\max} = 0.25\,\mathrm{h}^{-1}$; $K_S = 2.31\,\mathrm{mg/L}$; $X_0 = 820\,\mathrm{mg/L}$; $S_0 = 100\,\mathrm{mg/L}$; $\delta_{\mathrm{injection}} = 2.16\,\mathrm{s}$. (a) Dissolved oxygen profiles; the upper and the lower curves correspond to C_1 and C_2, respectively. (b) Substrate profiles at the initial stages of the injection. Remark the concentration discrepancy in the first minute caused by the different residence times in the aerobic (upper curve) and in the respiration chamber (lower curve). (c) Oxygen uptake rate (OUR) derived from curves plotted in (a) using equation (42b); the model (43) itself exhibits a transient not explained by the ASM models. (d) Detail of the OUR transient given by the model (43). The curves correspond at different flow rates, $Q = 48$, 38, 28 and 18 L/h, respectively; the rest of the parameters remain unchanged except $S_0 = 60\,\mathrm{mg/L}$.

Monod's standard model (see equations (17)–(19)) the slope of the OUR at $t = 0$ is given by:

$$\dot{R}_{\mathrm{exo}}(0) = \left.\frac{\partial R_{\mathrm{exo}}}{\partial t}\right|_{t=0} = -\frac{1-Y}{Y^2}\mu_{\max}^2 X_0^2 \frac{K_S}{(K_S+S_0)^3}\, S_0. \tag{53}$$

Since all the biokinetic constants are positive magnitudes, this expression is always negative. Nevertheless, calculating the slope of the OUR from equation (42d) we have:

$$\dot{R}_2(0) = \left.\frac{\partial R_2}{\partial t}\right|_{t=0} = \frac{1-Y}{Y}\mu_{\max} X_0 \frac{1}{K_S}\tau_2^{-1}\, S_0, \tag{54}$$

which always is positive. Then, again the model (42) explains better the transient at the beginning of the experiments. In figure 2d the calculated R_2 is shown at its initial stage. The slope of these curves are all positive which agree with the experimental observations [4]. The curves in figure 2d were plotted considering different flow rates between the two chambers of the respirometer. Using equation (54) it can be demonstrated that the slope of the curves at $t = 0$ is proportional to the flow rate and then, reducing this value, the slope of these curves decreases too. A lesser slope implies a longer transient, but as equation (54) suggests, the slope of these curves are the result of the interaction between the biokinetic process and the hydraulic set-up of the respirometer. Considering the intersection point of the asymptotes given by equations (53) and (54) an estimation of the duration of the transient could be derived:

$$\Delta_t = \frac{K_S\,(K_S + S_0)^2\;Y\;\tau_2}{(K_S + S_0)^3\;Y + K_S^2\;\mu_{max} X_0\;\tau_2} \sim \frac{K_S}{S_0}\;\tau_2. \tag{55}$$

5. Discussion

From the structural identifiability analysis of the models presented in this work it can be concluded that the determination of OUR is not compulsory for the determination of the biokinetic parameters which characterise the biological wastewater treatment processes. Moreover, it has been demonstrated that if the ODE's concerning the DO concentration are included in the mathematical model describing the dynamics of the respirometer, the measurement of the DO in the aerobic or in the respiration chamber are quite enough to obtain the biokinetic parameters of the model after fitting the DO data to the model. Under these circumstances the oxygen mass transfer coefficient and its saturation concentration could be calculated and consequently, it might be possible an accurate *a posteriori* determination of the OUR.

The thesis maintained along this work is that it is not possible to calculate the OUR with a respirometer prior to the knowledge of some parameters which only are accessible modelling the oxygen transfer process together with the biological processes, i.e. k_La and C^* (see equations (20), (42a) or (42b)). From a theoretical point of view, this problem concerns the convenience or not about considering the OUR or the DO as the state variables of the dynamical model that describes the respirometer. Although both magnitudes are related, this relationship is not symmetrical, nor equivalent. We can calculate the OUR from DO data but its inverse is not obvious, mainly in hybrid respirometers (see equations (42a) or (42b)).

If the state variables of a mathematical model change, the structural identifiability analysis of the model should be repeated in order to confirm its identifiable parameter groups. Conventionally, the identifiability analysis of activated sludge models were carried out considering the OUR as the known

observable magnitude of the system. Here and using different identifiability methodologies, it has been demonstrated that models which take into account the oxygen mass transfer and that use the DO as the state variable of the system, are an adequate representation of the respirometer to determine the biokinetic and the physical parameters of the model. In our work, we have tried to emphasize the advantages about working directly with the DO measurements. After all, it is obvious that using DO the errors associated to this magnitude are lower than those associated to OUR and consequently, it could have a beneficial effect on the reduction of the confidence intervals of the calculated biokinetic parameters.

The usual procedure for the determination of these parameters consists first in the calculation of OUR from DO whatever the hypothesis and simplifications are assumed in its determination and then, fitting the OUR data to a kinetic model using a non-linear regression fitting software. Thus, the errors associated to OUR calculation will be propagated to the calculated parameters affecting in the accuracy or in the confidence interval of them. Moreover, the structural identifiability analysis carried out in this work has demonstrated that the parameter groups theoretically identifiable using the DO as observable state variable are equal or similar to those identifiable using OUR.

Consequently, the same biokinetic parameters, or its groups, could be calculated using the raw experimental DO data after including in the model the differential equations associated to the oxygen mass transfer. It is obvious then that under these circumstances less errors are associated to data and thus, an improvement on the accuracy of the calculated parameters would be expected.

Furthermore, the problem of the transients observed in respirometers after a substrate injection has been analysed in this work. The explanation given here for this phenomenon, mainly in hybrid respirometers, is related to the discrepancy of the initial state in the aerobic and in the respiration chamber. As a result of this discrepancy, the rates R_1 and R_2, i.e. the OUR in both chambers, respectively, differ along all the experiment making difficult to interpret correctly the OUR data in a context where DO data are not included. Moreover, the coupling between the hydraulic and the biokinetic models has been confirmed deriving equation (55). In this expression, the mean hydraulic retention time appears coupled with the constants characterizing the Monod's model. Increasing the complexity of the hydraulic model, e.g. considering transport time-delays between the respiration and the aerobic chambers, new interactions can appear and longer transients could be generated. In conclusion, the determination of the biokinetic parameters with a respirometer implies to have a deep knowledge about the hydrodynamics of the instrument and its possible interaction with the biokinetic dynamics.

On the other hand, a deep analysis of the systematic errors associated to the DO measurement using Clark's electrodes might be necessary in the future. Remind that for the determination of the OUR it is almost necessary to evaluate the first derivative of the DO concentration respect the time. If we consider

that immediately after the substrate injection there is an abrupt depletion of the oxygen concentration in the aerobic chamber, the error in the determination of the first derivative of the DO at this point could be significant. This could be specially true if we consider that at the initial stages of the experiment, where the oxygen concentration changes very fast, the polymer membrane covering the Clark's electrode probably is not in a steady state. Thus, a detailed description of the measurement of DO just after the substrate injection will be necessary to evaluate the errors on OUR determination at this point.

However, even though the theoretical inconveniences for its determination, the OUR is still a valuable magnitude that should not be underestimate. Its main advantage is that provides an intuitive 'on-sight' measure of the microbiological activity in wastewater processes and then, it could be the basis to propose different biokinetic reaction mechanisms. What it was under discussion in this work was the appropriateness of the OUR to calibrate biokinetic models against other magnitudes such as the DO, not its substitution. Naturally, once the model has been calibrated and hence, the respirometer constants were accurately determined, it will be able to have a precise value for the OUR set in a clearly defined theoretical framework.

Acknowledgments

The authors acknowledge the Conselleria d'Empresa, Universitat i Ciència de la Generalitat Valenciana for the financial support to this work under the project Ref GV05/190.

References

[1] H. Spanjers, P.A. Vanrolleghem, G. Olsson and P.L. Dold, *Respirometry in Control of the Activated Sludge Process : Principles* (International Association on Water Quality, London, 1998).
[2] J.B. Copp, H. Spanjers and P.A. Vanrolleghem, *Respirometry in Control of the Activated Sludge Process : Benchmarking Control Strategies* (IWA Publishing, London, 2002).
[3] D. Dochain and P. Vanrolleghem, *Dynamical Modelling and Estimation in Wastewater Treatment Processes* (IWA Publishing, London, 2001).
[4] P.A. Vanrolleghem, G. Sin and K.V. Gernaey, Biotech. Bioeng. 86 (2004) 277–290.
[5] B. Petersen, K. Gernaey, M. Devisscher, D. Dochain and P.A. Vanrolleghem, Water Res. 37 (2003) 2893–2904.
[6] D. Dochain, P.A. Vanrolleghem and M. Vandaele, Water Res. 29 (1995) 2571–2578.
[7] M. Tayakout-Fayolle, E. Jolimaitre and C. Jallut, Chem. Eng. Sci. 55 (2000) 2945–2956.
[8] E. Walter and L. Pronzato, Math. Comp. Sim. 42 (1996) 125–134.
[9] K. R. Godfrey, *Compartmental Models and their Applications* (Academic Press, London, 1983).
[10] S. Vajda, K.R. Godfrey and H. Rabitz, Math. Biosci. 93 (1989) 217–248.
[11] N.D. Evans, M.J. Chapman, M.J. Chappell and K.R. Godfrey, Automatica 38 (2002) 1799–1805.
[12] R.L.M. Peeters and B. Hanzon, Automatica 41 (2005) 513–529.

[13] S. Audoly, G. Bellu, L. D'Angio, M.P. Saccomani and C. Cobelli, IEEE Trans. Biomed. Eng. 48 (2001) 55–65.
[14] G. Margaria, E. Riccomagno, M.J. Chappell and H.P. Wynn, Math. Biosci. 174 (2001) 1–26.
[15] M.J. Chapman, K.R. Godfrey, M.J. Chappell and N.D. Evans, Math. Biosci. 183 (2003) 1–14.
[16] M.J. Chapman, K.R. Godfrey, M.J. Chappell and N.D. Evans, Int. J. Control 76 (2003) 209–216.
[17] A. Raksanyi, Y. Lecourtier, E. Walter and A. Venot, Math. Biosci. 77 (1985) 245–266.
[18] P.A. Vanrolleghem and H. Spanjers, Water Sci. Technol. 37 (1998) 237–246.